Available online at www.sciencedirect.com
ScienceDirect
Applied Thermal Engineering 28 (2008) 145–156
Applied Thermal Engineering
www.elsevier.com/locate/apthermeng

Study on the mechanism of unsteady combustion related to volatile in a coal-fired traveling grate boiler

J.J. Ji *, Y.H. Luo, L.Y. Hu

Institute of Thermal Engineering, Shanghai Jiaotong University, Dongchuan Road 800, Shanghai 200240, PR China

Received 2 June 2006; accepted 25 March 2007
Available online 10 April 2007

Abstract

There are a variety of low-grade and hard-to-burn coals used in grate boilers in China. Almost all of them are manufactured with arches to promote the efficiency and their applicability to various coals. However, those boilers sometimes suffer from the unsteady combustion known as "puff", which degrades energy efficiency, emits smoke pollution and even damages components. The mechanism responsible for its occurrence has been speculated to be related to the abnormal combustion of volatile released from coal, however, the details have not been clearly known up till now.

In this paper, an experimental system is set up to investigate the unsteady combustion mechanism in an industrial traveling grate boiler. Natural gas is used to simulate the volatile from coal. Under the condition of two typical air distribution modes, dynamic pressure signals at various flow rates with fixed stoichiometric ratio are measured and influence factors on the unsteady combustion are studied. The detailed combustion characteristics are analyzed with large eddy simulation. The simulation is in reasonable agreement with the experiment and further discovers the mechanism of the volatile-related unsteady combustion. Moreover, the frequency analysis of the experimental data also confirms this mechanism.

Keywords: Traveling grate boiler; Coal-fired; Unsteady combustion; Puff; Pressure fluctuation

1. Introduction

There are more than 500,000 industrial boilers in China [1], consuming about one third of the total nationwide coal consumption. Most of these industrial boilers are coal-fired grate boilers. The coal used in these grate boilers is mostly raw coal without size grading, much less briquetting and washing. On the other hand, the coal quality for an industrial boiler is sometimes changeable due to the variety in coal quality of different coalmines. All these facts make the coals difficult to ignite and burn out.

To promote the efficiency of grate boilers and their applicability to various coals, most of these grate boilers are manufactured with arches to optimize combustion. There are usually two arches over the grate in the furnace, the front arch and the rear arch. The main function of the front arch is to radiate heat on the new coal entering the furnace, which guarantees the ignition; the rear arch keeps the high local temperature and thus promotes the burnout of the coal. Moreover, the appropriate match between the front arch and the rear arch can improve the mixing of the air and the combustible gas, which reduces the combustible gas loss.

There are a variety of arch types in harmony with the various coals in China. In order to burn low-grade coals, Chinese researchers have developed several novel arches, such as the α-shaped arch [2], the vortex arch [3] and the double-herringbone arch [4].

The pressure in a furnace is usually required to keep slightly negative under the normal operation condition, about $-20 \sim -30$ Pa. But a grate boiler sometimes may suffer from a kind of unsteady combustion known as "puff", which makes the pressure in the furnace rise above

* Corresponding author. Tel.: +86 21 34205702; fax: +86 21 34206115.
E-mail address: junjieji@gmail.com (J.J. Ji).

1359-4311/$ - see front matter
doi:10.1016/j.applthermaleng.2007.03.031

Nomenclature

C_s	Sm agorinsky constant
d	distance to the closest wall (m)
f	mixture fraction
H	total enthalpy (J kg^{-1})
L_s	mixing length for sub-grid scales (m)
M_j	sub-grid scale mass flux of mixture fraction (kg m^{-2} s)
M-T	mixed-type air distribution
p	pressure (Pa), or probability density function
PDF	probability density function
Pr	Prandtl number
Q_j	sub-grid scale thermal energy flux (W m^{-2})
Sc	Schmidt number
$\overline{S}_{ij}$	rate of strain tensor for the resolved scale (s^{-1})
S_j	sub-grid term in the generic governing equation
S_r	source term due to radiation (W m^{-3})
SR	stoichiometric ratio
S-T	separated-type air distribution
S_ϕ	source term in the generic governing equation
t	time (s)
u	velocity (m s^{-1})
V	volume of a computational cell (m^3)
x	coordinate vector

Greek symbols

α,β	parameters in β function
δ_{ij}	Kronecker delta function
κ	von Kármán constant
μ	dynamic viscosity (Pa s)
ϕ	generic variable
ρ	density (kg m^{-3})
σ_{ij}	molecular strain rate tensor
τ_{ij}	sub-grid scale stress

Subscripts

i, j, k	cartesian components; coordinates
t	sub-grid scale coefficient

Superscripts

$-$	filtered variable
$'$	sub-grid scale variable

the atmospheric pressure. Such unsteady combustion is a common phenomenon in grate boilers with arches, which can result in efficiency drop, smoke pollution and component damage. However, the occurrence mechanism and whether it is related to the various coals and arches are not clearly known.

In an effort to understand the unsteady combustion, a number of studies have been performed during the past few years. Hui et al. [5] found that "puff" is a common phenomenon in grate boilers with arches. There may be a relationship between "puff" and arches. Huang et al. [6] further discovered following features.

(1) They mainly occur when high volatile coal is burnt;
(2) They are related to the air distribution mode under the grate;
(3) Sparks and smoke spurt from the furnace intermittently (Fig. 1).

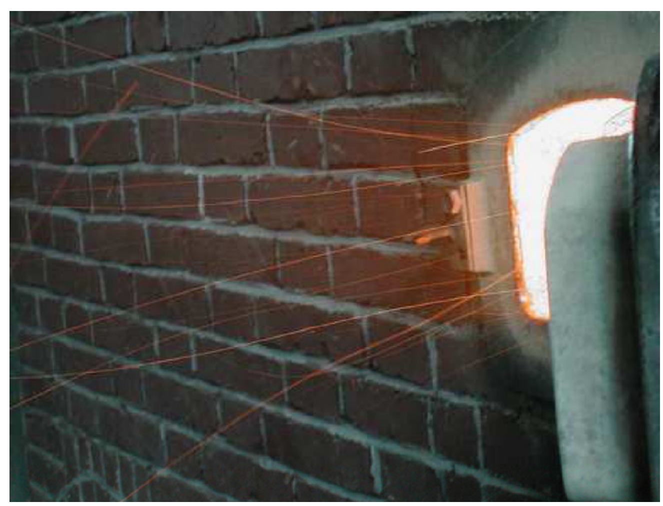

Fig. 1. Sparks and smoke spurting from the furnace as a phenomenon of "puff".

Considering the above features, Huang et al. [6–8] speculated that there must be an intrinsic relationship between such unsteady combustion and the abnormal combustion of the volatile from coal.

In this paper, an experimental grate boiler model is established to simulate an industrial traveling grate boiler with arches in which the unsteady combustion occurs. Natural gas is used to simulate the volatile. Under two typical air distribution modes, the magnitudes of dynamic pressure fluctuations at various flow rates are studied to determine influence factors on the volatile-related unsteady combustion. Large eddy simulation is used to study the vorticity and combustible gas profile in the furnace under the two air distribution modes so as to understand the occurrence mechanism. Moreover, frequency characteristics of the measured pressure fluctuations are analyzed for the further investigation on the mechanism.

The paper is organized in the following manner: The first section briefly describes the experimental facility and measurement scheme, and second the LES model and the numerical settings adopted in the simulation. Then, the experimental and simulated results are given and the mechanism of the volatile-related unsteady combustion is discussed. Finally, the frequency characteristics of experimental data are investigated, going with some discussions on them.

2. Experimental set-up and measurement scheme

2.1. Experimental set-up

In this study, a real traveling grate boiler in which the volatile-related unsteady combustion occurs is chosen as the prototype of the experimental combustor. The size of the experimental combustor is one tenth of the real furnace size. Natural gas is used to simulate the volatile.

As is shown in Fig. 2, the width of the combustion chamber is 220 mm and the height of it is about 600 mm. The wall is made of the refractory material with a thickness of 100 mm. Air and natural gas are fed from the grate. There are six rooms under the grate. Every room has three air pipes at uniform intervals. Air flows from the holes bored directly upwards in the air pipes. The flow rate of every pipe in one room is the same. Various air distribution modes can be established by adjusting volume fluxes of the air pipes. Partition plates are fixed between adjacent rooms.

Natural gas enters the combustion chamber through a perforated plate under the front four rooms. Since the volatile distribution along the grate length increases first and then decreases until zero in the real traveling grate boiler, the plate has 220 holes of 20 columns and 11 rows to distribute natural gas so as to simulate the volatile distribution feature. The diameters of the holes in one row are the same. The diameters of the holes in the column direction (corresponding to the grate length direction of the industrial furnace) are shown in Fig. 3.

A 20 mm thick layer of ceramic pebbles with hydraulic diameters of 10–15 mm is supported directly by the grate made of a stainless steel net. The ceramic pebbles simulate the coal on the grate and stabilize the flame.

The pipeline of the air supply subsystem is also shown in Fig. 2. Air is supplied through a Roots blower. Six main air ducts are connected to the pressure stabilizer and every main duct furcates into three air pipes in every room. Pitot tubes in the main ducts are used to measure the flow rates. Compressed natural gas tanks provide the natural gas and the flow rate is measured by a rotameter. The natural gas is mainly composed of methane, whose volume fraction is 91.4% (measured by a Shimadzu GC-14B gas chromatograph).

The pressure signals are recorded by a dynamic pressure sensor (model 106B51) made by PCB company (USA). The resolution of the sensor is 0.34 Pa and the low frequency response of it is 0.5 Hz. The data are input into the computer via the sampling of the data acquisition board (model AD8201, Chinese RBH Inc.) and the amplification of the signal conditioner (model 480E09, PCB Inc.). The sampling frequency is 1000 Hz.

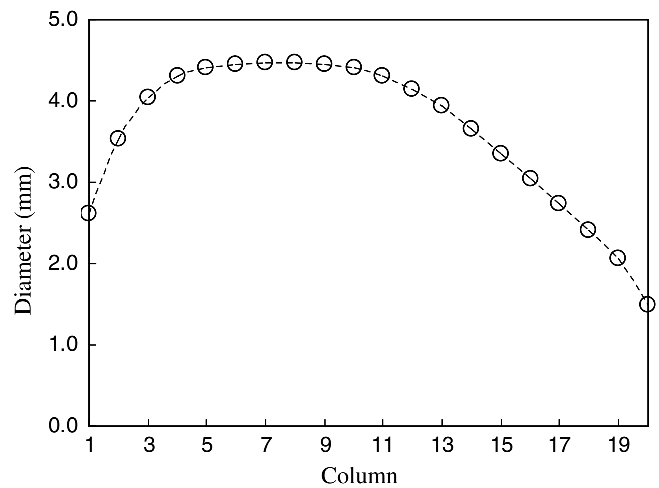

Fig. 3. Diameters of the holes in the perforated plate in the column direction.

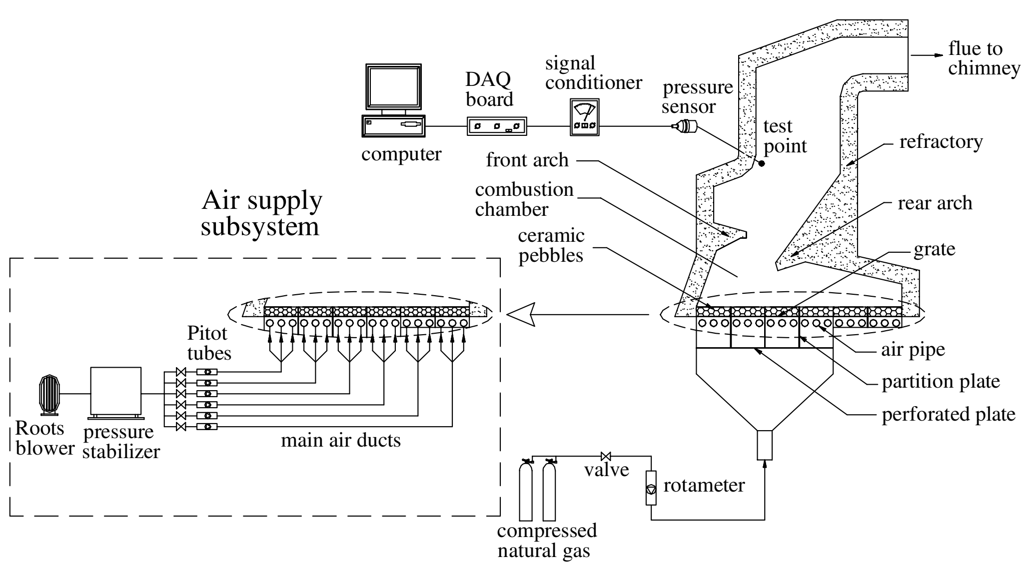

Fig. 2. Schematic of the experimental system.

2.2. Experimental scheme

Two typical air distribution modes are adopted in the experiment for comparison. One is the mixed-type air distribution (abbreviated to M-T), that is, the air and the natural gas are supplied to the chamber from the same rooms, which makes the air and the natural gas mix well, as is shown in Fig. 4, where the volume flux distribution of the natural gas is calculated according to the diameters of the holes in the perforated plate; The other is the separated-type air distribution (abbreviated to S-T), that is, the air and the natural gas enter the combustion chamber from different rooms, which results in the poor initial mixing of them.

To study the influence of M-T and S-T on the unsteady combustion, pressure fluctuations at different flow rates under these two air distribution modes are measured. The detailed scheme is shown in Table 1, which can be divided into two parts:

1. Combustion at different flow rates: test 1∼ test 3 in the table with the same stoichiometric ratio 2.0. The influence of flow rate is also studied in this part;
2. Cold flows: test 4–test 6 in the table. This part is the baseline to investigate the contribution of the volatile chemical energy to pressure fluctuations by comparing the cold flows with the combustion.

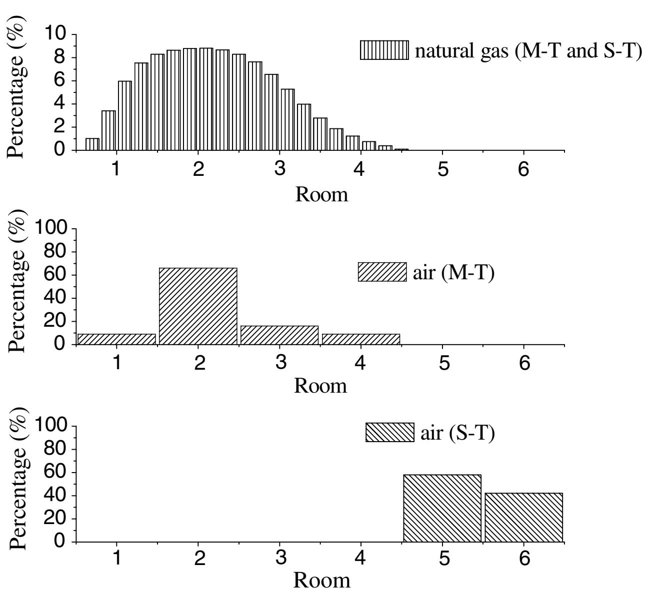

Fig. 4. Volume flux distribution of the natural gas and the air of the two air distributions (M-T and S-T).

Table 1
Scheme of the experiment (M-T and S-T are adopted for each test)

Test	State	Stoichiometric ratio	Flow rate (m^3/h)
1	Combustion	2.0	12.6
2	Combustion	2.0	25.3
3	Combustion	2.0	52.6
4	Cold flow	–	12.0
5	Cold flow	–	24.0
6	Cold flow	–	50.0

3. LES model and numerical method

Large eddy simulation (LES) is adopted to study the combustion characteristics of the two air distribution modes in the experiment. Although a real vortex is always three dimensional, two-dimensional large eddy simulation (2D LES) is used here for the simplification according to the flow field characteristics of the traveling grate boiler. The Smagorinsky-Lilly sub-grid turbulence model and the non-premixed (PDF) combustion model are used. Running a case on a PC workstation with a 2GB RAM and double 3.0 G CPU needs about 2 days to make the flow field approaching a statistical steady state.

In the LES, the spatially filtered value $\bar{\phi}$ of a variable ϕ is defined as

$$\bar{\phi}(x) = \frac{1}{V}\int_V \phi(x')\,\mathrm{d}x', \quad x' \in V \tag{1}$$

where V is the volume of a computational cell, and x is the coordinate vector.

Ignoring the density pulsation, a generic form of the filtered governing equations can be written as

$$\frac{\partial(\rho\bar{\phi})}{\partial t} + \frac{\partial(\rho\bar{u}_j\bar{\phi})}{\partial x_j} = -\frac{\partial S_j}{\partial x_j} + S_\phi \tag{2}$$

where S_j is the sub-grid term, and S_ϕ is the source term. The detailed expressions for S_j and S_ϕ in the generic equation are shown in Table 2, where σ_{ij} is the molecular strain rate tensor.

$$\sigma_{ij} = \mu\left(\frac{\partial\bar{u}_i}{\partial x_j} + \frac{\partial\bar{u}_j}{\partial x_i}\right) - \frac{2}{3}\mu\frac{\partial\bar{u}_k}{\partial x_k}\delta_{ij} \tag{3}$$

The sub-grid scale stress τ_{ij} is defined by

$$\tau_{ij} \equiv \rho\overline{u_i u_j} - \rho\bar{u}_i\bar{u}_j \tag{4}$$

Smagorinsky–Lilly model [9,10] is employed to close τ_{ij}.

$$\tau_{ij} = \frac{1}{3}\tau_{kk}\delta_{ij} - 2\mu_t\overline{S}_{ij}, \quad \mu_t = \rho L_s^2\sqrt{2\overline{S}_{ij}\overline{S}_{ij}}$$

where μ_t is the sub-grid scale (SGS) eddy-viscosity, and L_s is the mixing length for sub-grid scales. $\overline{S}_{ij}$ is the rate of strain tensor for the resolved scale defined by

$$\overline{S}_{ij} = \frac{1}{2}\left(\frac{\partial\bar{u}_i}{\partial x_j} + \frac{\partial\bar{u}_j}{\partial x_i}\right) \tag{5}$$

Table 2
Detailed expressions for S_j and S_ϕ in the generic governing equation

Equation	ϕ	S_j	S_ϕ
Continuity	1	0	0
Momentum	u_i	τ_{ij}	$-\frac{\partial p}{\partial x_i} + \frac{\partial\sigma_{ij}}{\partial x_j}$
Energy	H	Q_j	$\frac{\partial}{\partial x_j}\left(\frac{\mu}{Pr}\cdot\frac{\partial\overline{H}}{\partial x_j}\right) + S_r$
Mixture fraction	f	M_j	$\frac{\partial}{\partial x_j}\left(\frac{\mu}{Sc}\cdot\frac{\partial\bar{f}}{\partial x_j}\right)$

L_s is computed using

$$L_s = \min(\kappa d, C_s V^{1/3}) \tag{6}$$

where κ is the von Kármán constant (=0.4187) [11,12], d is the distance to the closest wall, C_s is the Smagorinsky constant (0.16) [13].

The sub-grid scale thermal energy flux Q_j and the sub-grid scale mass flux of mixture fraction M_j are simply modeled [13] as

$$Q_j = -\frac{\mu_t}{Pr_t}\frac{\partial \overline{H}}{\partial x_j}, \quad M_j = -\frac{\mu_t}{Sc_t}\frac{\partial \bar{f}}{\partial x_j}$$

where Pr_t and Sc_t are assumed to be constant. $Pr_t = Sc_t = 0.7$ [14,15].

The mixture fraction variance $\overline{f'^2}$ is not solved with a transport equation, but directly modeled as

$$\overline{f'^2} = \frac{1}{2} L_s^2 |\nabla \bar{f}|^2 \tag{7}$$

βfunction is assumed as the PDF shape, given by the following function of $\bar{f}$ and $\overline{f'^2}$

$$p(f) = \frac{f^{\alpha-1}(1-f)^{\beta-1}}{\int f^{\alpha-1}(1-f)^{\beta-1}\,\mathrm{d}f} \tag{8}$$

where α and β are all the function of $\bar{f}$ and $\overline{f'^2}$

$$\alpha = \bar{f}\left[\frac{\bar{f}(1-\bar{f})}{\overline{f'2}} - 1\right], \quad \beta = (1-\bar{f})\left[\frac{\bar{f}(1-\bar{f})}{\overline{f'^2}} - 1\right]$$

Then, mean species mass fractions or temperature $\overline{\phi_i}$ are achieved by

$$\overline{\phi_i} = \int_0^1 \phi_i(f, \overline{H}) p(f)\,\mathrm{d}f \tag{9}$$

Thus, the look-up table, which is the function of $\bar{f}$, $\overline{f'^2}$, and enthalpy $\overline{H}$, is constructed.

$$\overline{\phi_i} = \overline{\phi_i}(\bar{f}, \overline{f'^2}, \overline{H}) \tag{10}$$

Table 3
Simulation settings

Items	Scheme
Method	Finite volume method (FVM)
Solver	Segregated implicit
Temporal discretization	Second order
Pressure	PRESTO!
Momentum equation	QUICK
Other equations	Second order upwind
Pressure–velocity coupling	PISO
Inlet boundary condition	Velocity inlets
Outlet boundary condition	Pressure outlet (0 Pa)
Wall condition	Constant temperature (500 K), constant emissivity (0.8)
Cell type	Quadrilateral paved grid
Total cells amount	12,900
Time step	0.0002 s

The natural gas is assumed as pure methane in the simulation, for the main species in the natural gas is CH_4. The intermediate species decomposed from methane, i.e. CO, H_2, and C(s) and the products, i.e. CO_2, H_2O are included. The concentration sum of CH_4, CO and H_2 is regarded as the concentration of combustible gas in the combustion chamber. P-1 model [16,17] is used for radiation. The Weighted-Sum-of-Gray-Gases Model [18,19] is chosen to calculate the absorption coefficient. The numerical simulation settings are shown in Table 3.

4. Results and discussion

4.1. Magnitude analysis

Since the unsteady combustion is caused by large magnitude pressure fluctuations of combustion, magnitude analysis of the experimental data are used to study the influence factors on the unsteady combustion in this section. The magnitude of a dynamic pressure signal is estimated by its standard deviation, that is

$$\mathrm{SD} = \sqrt{\frac{1}{n-1}\sum_{i=1}^{n}(p_i - \bar{p})^2} \tag{11}$$

where $\bar{p}$ is the mean pressure; p_i is the pressure data point; n is the total number of the pressure data points.

Typical pressure signals measured in the experiment are given in Fig. 5, where (a) and (b) show the pressure signals of the cold flow for M-T and S-T at 50 m^3/h (test 6 in Table 1), (c) and (d) showing the combustion pressure signals for M-T and S-T at 52.6 m^3/h (test 3 in Table 1), respectively. Using standard deviation, the magnitudes for the two air distribution modes at the three flow rates are summarized in Fig. 6.

It can be seen from Figs. 5 and 6 that: (1) the combustion pressure magnitudes are much larger than those of cold flows, which are all close to zero; (2) the pressure magnitudes of the cold flows almost have no relation with the flow rate, however, the combustion pressure magnitudes increase with the increasing of flow rate; (3) combustion pressure magnitudes of S-T are much larger than those of M-T at any flow rates we tested. And this trend is more obvious with the increasing of flow rate.

Based on the above three results, some influence factors on the unsteady combustion are analyzed as follows:

(1) *Volatile chemical energy*
According to aerodynamics, the slight pressure fluctuations in the cold flows are caused by the unavoidable turbulent noise and the periodic vortex shedding behind bluff bodies. However, as far as the combustion is concerned, there is not only fluid flow but also the reaction between the fuel and the air. The reaction will release heat and do expansion work, which causes pressure disturbance in the furnace. As a result, it can be concluded that pressure fluctuations

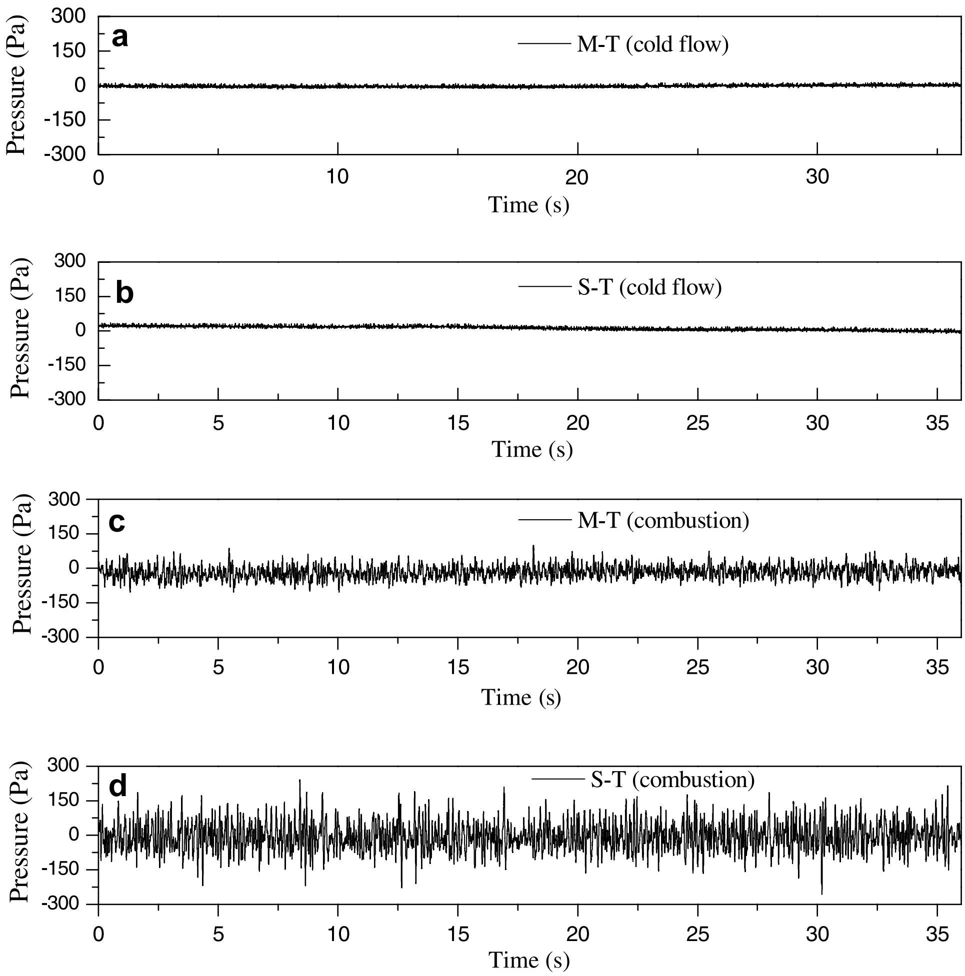

Fig. 5. Typical dynamic pressure signals: (a) cold flow, M-T at 50 m^3/h; (b) cold flow, S-T at 50 m^3/h; (c) combustion, M-T, 52.6 m^3/h, SR = 2; and (d) combustion, S-T, 52.6 m^3/h, SR = 2.

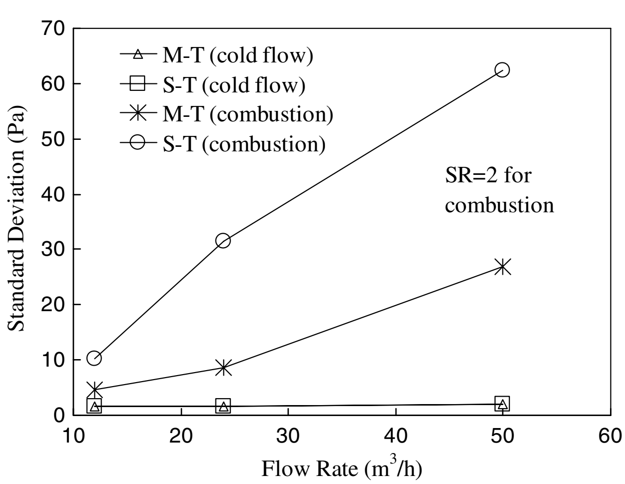

Fig. 6. Standard deviations of dynamic pressure fluctuations at various flow rates.

will be largely enhanced if there is fuel combustion. Therefore, volatile chemical energy does a much greater contribution to the unsteady combustion than aerodynamic instability does, which confirms forego-ing Huang's speculation [6,7].

(2) *Flow rate*
In cold flows, larger flow rate only leads to intenser turbulence and vortex shedding. The change in the pressure fluctuation magnitude is imperceptible. However, the combustion pressure magnitudes increase remarkably with the increasing of flow rate, owing to the fact that larger flow rate of combustion results in more combustible gas and more chemical energy for the reaction. Since larger boiler load implies larger flow rate, larger boiler load makes the unsteady combustion easier to occur.

(3) *Air distribution mode*
The combustion pressure magnitudes of S-T are much larger than those of M-T independent of flow rate, indicating that poor initial mixing between the volatile and the air leads to larger pressure fluctua-tions than good initial mixing does. Therefore, for those air distributions similar to S-T in a real travel-ing grate boiler, if the volatile releases plentifully from coal and there is not enough air there, great

pressure fluctuations will yield, which may lead to "puff".

4.2. Numerical simulation results

The above experimental results imply that poor initial volatile-air mixing makes the unsteady combustion occur easily. To understand the mechanism, the typical combustion under the two air distribution modes (M-T and S-T) whose pressure fluctuations are previously shown in Fig. 5(c) and (d) is simulated for comparison.

The simulated combustion pressure fluctuations of M-T and S-T are shown in Fig. 7. (The frequency seems higher than that of the experiments because that the calculation time step must be set smaller than the experiment time resolution in order to achieve convergence within each iteration.) The simulation result also shows that the combustion pressure magnitude of S-T is much larger than that of M-T. The pressure magnitude of M-T is about 30 Pa, close to the data recorded in the experiment (Fig. 5). And the pressure magnitude of S-T is about 200 Pa, a little larger than the experiment result but acceptable for the quality analysis of the mechanism.

The evolution of the vorticity and the combustible gas mole fraction of the combustion for S-T are shown in Fig. 8, where the vorticity is denoted by the contour lines and the combustible gas mole fraction is indicated by the flooded contour. In the figure, the combustible gas mole fraction is calculated as the mole fraction sum of CH_4, CO and H_2. As can be seen, the vortexes are rolling up from the noses of the front arch and the rear arch. But, the combustible gas is only in the vortex core shedding from the front arch nose. Furthermore, combustible gas enveloped in the shedding vortex is transported downstream until it impinges on the wall and breaks up into smaller vortexes.

The simulated vorticity and temperature map for S-T during vortex shedding stage are shown in Fig. 9. And the pressure field when the vortex breaks up is shown in Fig. 10. The temperature is high on the border of vortexes and low in vortexes core, which means that the reaction mainly occurs on the border of vortexes where the combustible gas and the oxygen meet. The combustible gas enveloped in vortexes is difficult to react with the oxygen around the vortexes in the process of vortex shedding. But when the vortex breaks up, the wrapped combustible gas is to release and quickly react with the surrounding oxygen, which leads to a pressure source around the impinging point (see Fig. 10).

The simulated results for M-T (Fig. 11) show that there are also vortexes shedding in the chamber, but the combustible gas burns out before it reaches the front arch nosedue to the good initial mixing. Thus, there is no remarkable pressure disturbance like that in S-T.

4.3. Mechanism of the unsteady combustion

As is shown in the experiment and the simulation, the vortex shedding and the volatile chemical energy play important roles in the occurrence of the unsteady combustion. Thus, the detailed mechanism is concluded in Fig. 12, which can be described in the following stages:

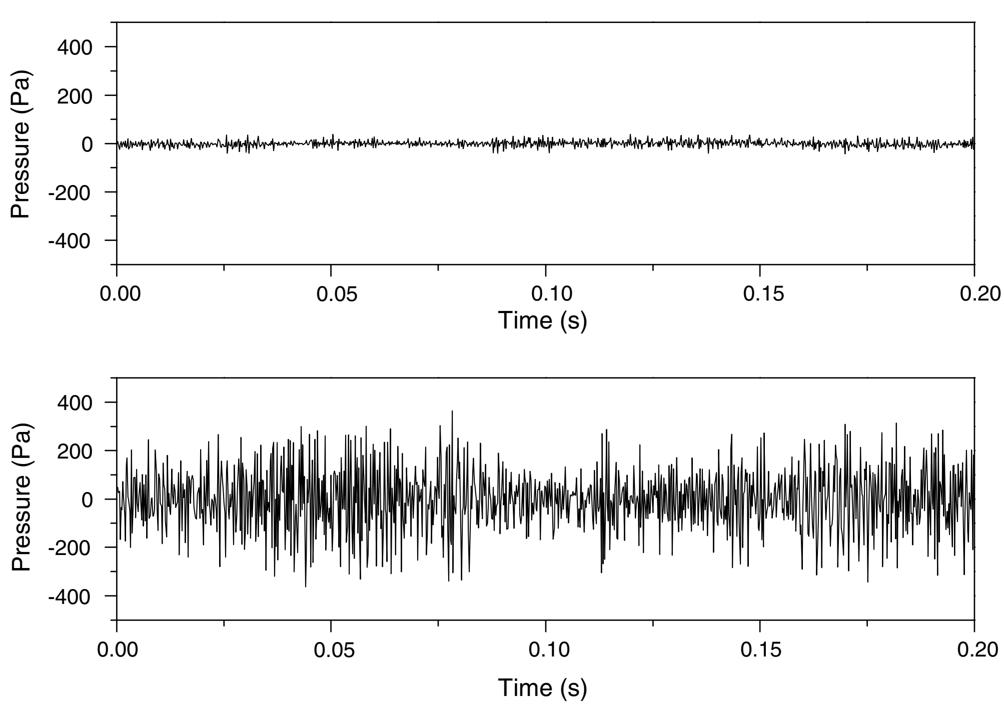

Fig. 7. Simulated combustion pressure fluctuations of M-T and S-T, flow rate = 52.6 m^3/h, SR = 2.

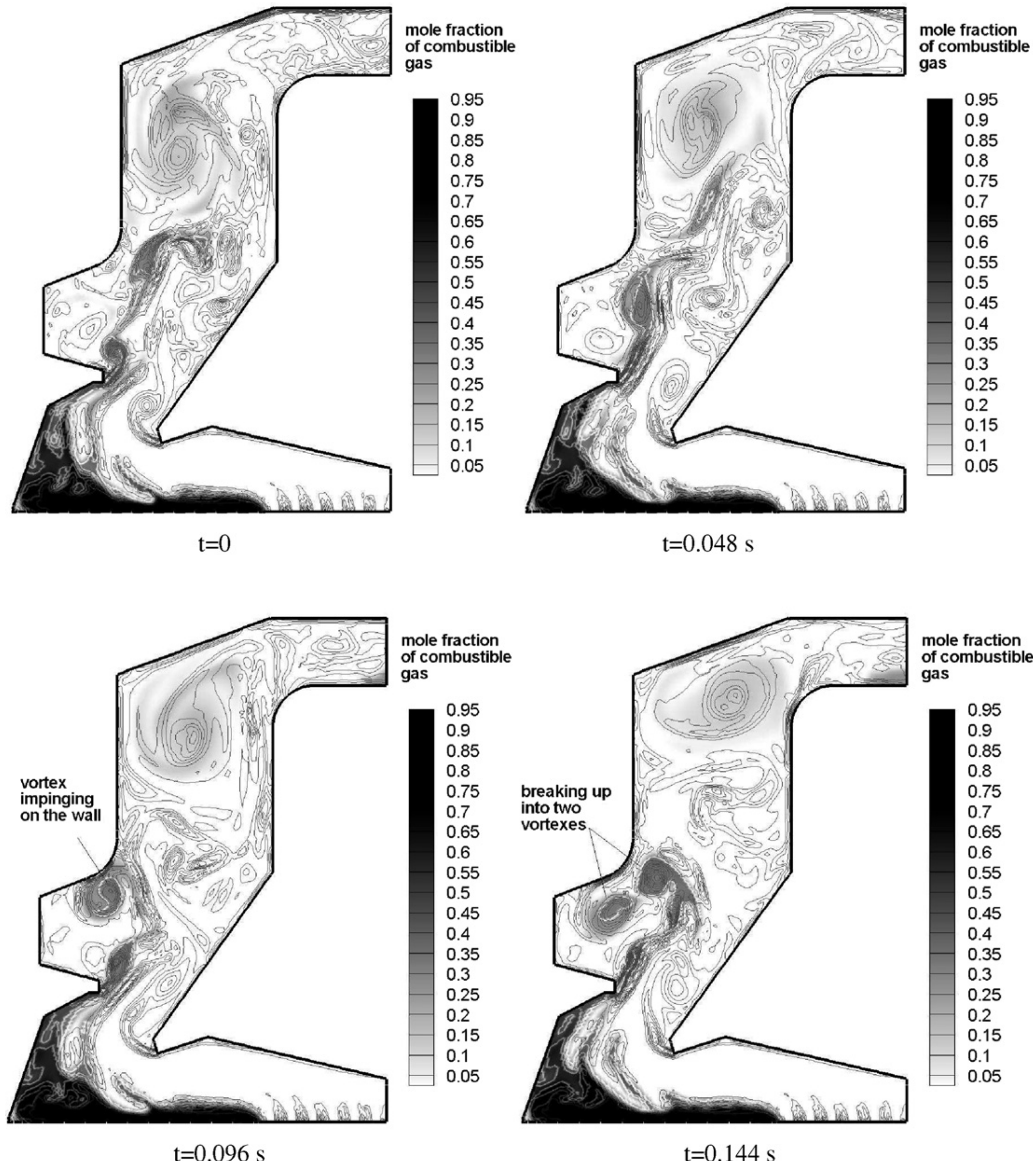

Fig. 8. Simulated vorticity evolution and combustible gas mole fraction of S-T, flow rate = 52.6 m^3/h, SR = 2.

(1) Aerodynamic instability is unavoidably caused by the turbulence and periodic vortex shedding from the noses of arches, which can lead to slight pressure fluctuations whose magnitude, however, is very small and can be neglected.
(2) Volatile releases largely from the coal under the front arch. If the air distribution cannot make the air initially mix well with the volatile, more volatile will not burn out steadily before it arriving at the nose of the front arch and consequently be entrained in the vortexes shedding from the front arch. Once the volatile is involved in vortexes, it is difficult to react with the outer oxygen and its combustion is depressed. Thus, there exists plenty of unburnt volatile in the vortex core in the process of vortex growing up.
(3) When the vortexes impinge on the wall, they will break up into small-scale structures. The enveloped volatile is thus released and quickly reacts with the surrounding oxygen due to the high temperature in the combustion chamber. As a result, the pressure in the furnace rises abruptly because of the great contribution of volatile chemical energy to pressure fluctuations and thus the intermittent "puff" occurs.

Furthermore, some influence factors on the volatile-related unsteady combustion are discussed as follows according to the above mechanism:

(1) Configuration of arches: Since the volatile usually releases largely from the front of the grate but little

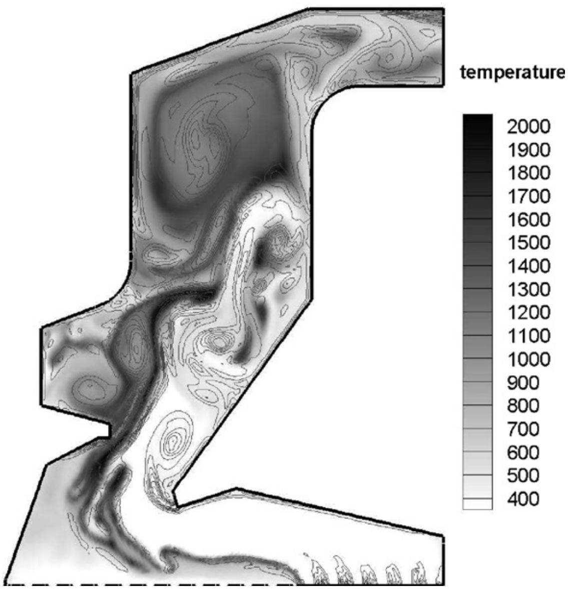

Fig. 9. Simulated vorticity and temperature of S-T (at $t = 0.048$ s in Fig. 8), flow rate = 52.6 m^3/h, SR = 2.

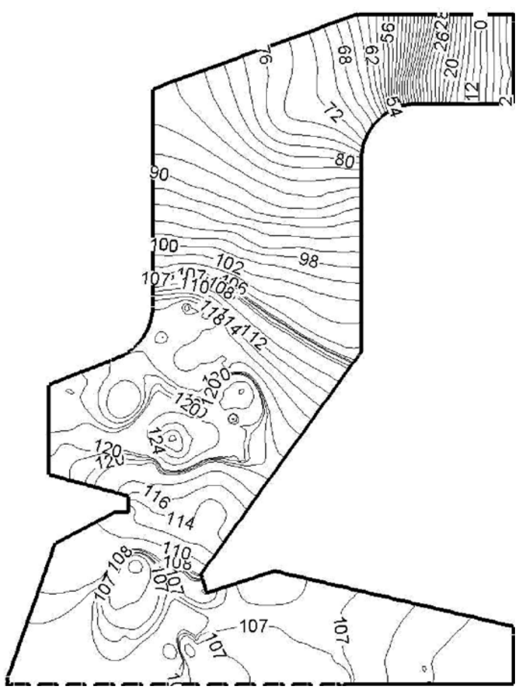

Fig. 10. Simulated pressure distribution of S-T (at $t = 0.144$ s in Fig. 8), flow rate = 52.6 m^3/h, SR = 2.

at the rear of the grate, and the air supply at the rear is usually excessive, the unsteady combustion is generally induced by the front arch. On the other hand, the shape of the rear arch influences on the characteristic of vortexes shedding from the front arch. Furthermore, it transports flue gas abundant in oxygen to the front area where the unsteady combustion originates. Therefore, the design of arches is a key factor to the unsteady combustion and will be an important issue in further investigations to control it in grate boilers.

(2) Volatile content in coal: In the combustion of coal with higher volatile, more volatile is released and entrained in vortexes, thus greater pressure fluctuation will yield, leading to more occurrence probability of the unsteady combustion.
(3) Air distribution: Poor volatile-air mixing makes more volatile unburnt before it arriving at the nose of the front arch. As a result, more volatile is enveloped in vortexes and larger magnitude of pressure fluctuation is produced.
(4) Boiler load: Larger boiler load means more coal input and more volatile release, which enlarges the pressure fluctuation magnitude. Second, larger boiler load leads to higher flow speed and thus less residence time before the volatile arriving at the nose of the front arch. As a result, more volatile is unburnt and entrained in vortexes, inducing larger magnitude of pressure fluctuation.

4.4. Frequency analysis

Pressure fluctuation frequency contains the combustion information, indicating the distribution of periodic components that synthesize the pressure signal. The frequency spectrum of the typical case whose pressure fluctuations are previously shown in Fig. 5 is analyzed and discussed in this section.

The spectrum density function of the measured pressure signals of the cold flows is shown in Fig. 13a. For M-T, the basic frequency of 2 Hz and the second harmonic of 4 Hz can be clearly seen, revealing the periodicity of the pressure fluctuation. Researches [20,21] have shown that vortex shedding leads to periodic pressure fluctuations in cold flows. Therefore, the frequency of 2 Hz is caused by periodic vortex shedding from arches. On the other hand, the frequency peaks of the S-T pressure fluctuation are also 2 Hz and 4 Hz. There is almost no difference between S-T and M-T in the frequency peak distribution.

The spectrum density functions of the measured pressure signals of the combustion for M-T and S-T are shown in Fig. 13b. There is more combustion noise compared with the cold flows. And the peaks of the spectrum density function for M-T are dispersed, indicating the noise of various frequencies. However, the frequency peaks of S-T are concentrated. The main peak can be identified, that is about 8 Hz. The reason may be as follows according to the mechanism of the unsteady combustion related to volatile.

In the cold flow, there are vortexes shedding in both M-T and S-T. In addition, the flow rate and the arches of M-T and S-T are the same. According to aerodynamics, vortex shedding frequency is determined by mean flow

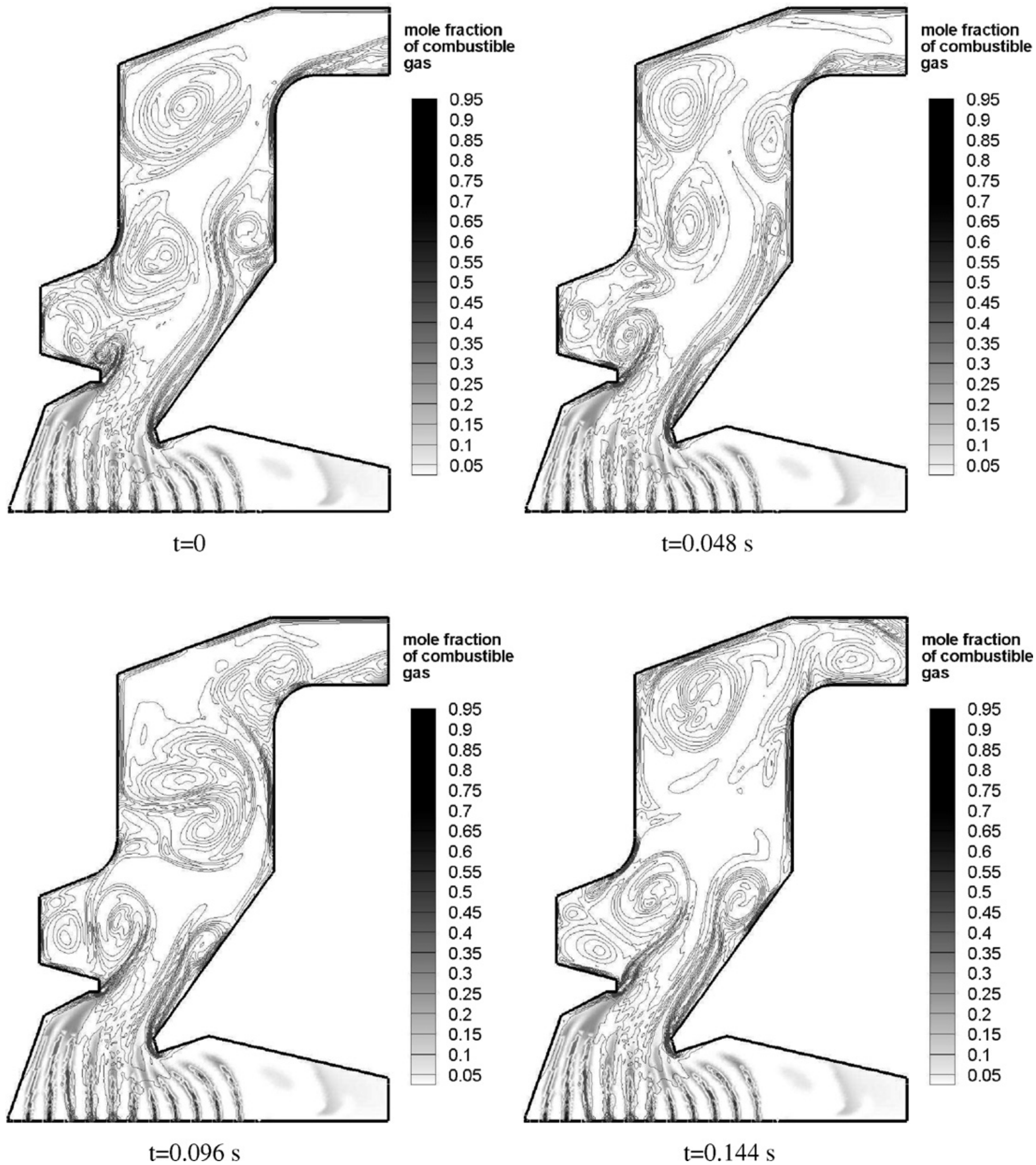

Fig. 11. Simulated vorticity evolution and combustible gas mole fraction of M-T, flow rate = 52.6 m^3/h, SR = 2.

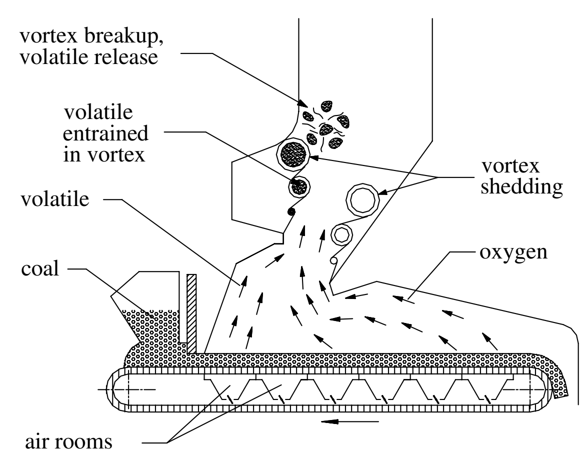

Fig. 12. Schematic of the mechanism of the volatile-related unsteady combustion.

velocity and structure dimension at a certain Reynolds number [22]. Therefore, the frequency characteristic of the cold M-T flow is almost the same as that of the cold S-T flow.

In the combustion, there are also periodic vortex shedding in M-T and S-T. However, due to the fact that the contribution of fuel chemical energy to pressure fluctuations is much larger than that of aerodynamic instability, whether there is periodicity in the pressure fluctuations is mainly determined by the feature of fuel combustion. In S–T, the periodic vortex shedding and breakup may induce periodic fast reaction between the volatile and the oxygen and thus periodic pressure raise, which is strong because of the chemical energy release, and therefore pressure fluctuations show periodicity. Whereas, for M-T, the only factor that can cause periodic pressure fluctuation is the pure

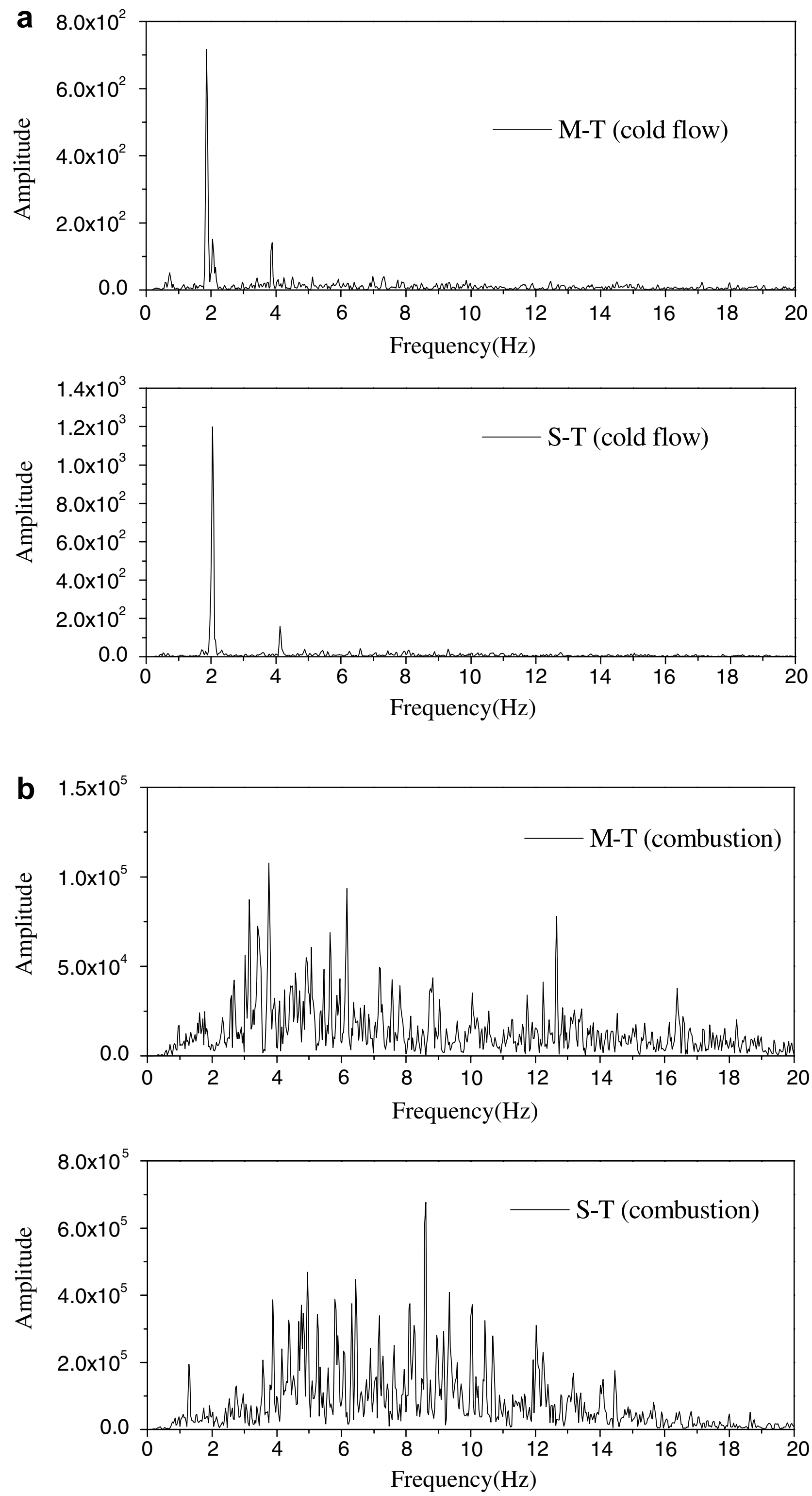

Fig. 13. Pressure spectrum density function of (a) cold flows and (b) combustion; flow rate = 50 m^3/h for cold flows, flow rate = 52.6 m^3/h and SR = 2 for combustion.

vortex shedding (without the periodic abrupt pressure raise when vortexes break up) and it is much weaker than the combustion noise and thus is concealed by the combustion noise of various frequencies.

5. Conclusions

An experimental system is established to simulate the traveling grate boiler in which the volatile-related unsteady combustion occurs. Dynamic pressure signals at various flow rates with fixed stoichiometric ratio 2.0 under the two air distribution modes, M-T and S-T, are measured and analyzed with their magnitudes. The difference in the combustion features between M-T and S-T is studied by large eddy simulation. As a result, the mechanism of the unsteady combustion and some influence factors are obtained. Finally, frequency characteristics of M-T and S-T are compared for further investigation on the mechanism. The detailed conclusions are as follows:

1. The "puff" is confirmed to be caused by the unsteady volatile combustion induced by the vortexes shedding from the front arch. Volatile is usually abundant under the front arch and if there is not enough air, volatile will be entrained in vortexes shedding from the nose of the front arch. In this process, the volatile combustion is depressed. When vortexes break up, the enveloped volatile will quickly react with outer oxygen, leading to great pressure fluctuations and the resultant unsteady combustion.
2. The unsteady combustion lies on the configuration of arches. Since the vortex shedding from the front arch is the source of the unsteady combustion, and the rear arch influences the flow field including the vortex shedding, the configuration of arches is critical.
3. The unsteady combustion is related to coal type and boiler load. Higher volatile coal and larger boiler load make more volatile to be involved in vortexes and therefore greater pressure fluctuations yield when vortexes break up, which promotes the occurrence of "puff".
4. The unsteady combustion depends on the air distribution. Poor initial volatile-air mixing makes the volatile less burnt out before it reaches the nose of the front arch and more volatile is entrained in vortexes. Therefore, the unsteady combustion is easy to occur when initial volatile-air mixing is poor.

References

[1] J.H. Fang, T.F. Zeng, L.I.S. Yang, et al., Coal utilization in industrial boilers in China – a prospect for mitigating CO_2 emissions, Applied Energy 63 (1) (1999) 35–52.

[2] S.E. Hui, T.M. Xu, Z.J. Liu, et al., A new method for designing the grate firing furnace arch with a highly turbulent α-shaped combustion flame, Reneng Dongli Gongcheng/Journal of Engineering for Thermal Energy and Power 9 (5) (1994) 280–284 (in Chinese).

[3] Z.N. Zhuang, C.X. Zhu, G.H. Tang, A study of the features of a novel vortex arch suited for the combustion of anthracite coal, Reneng Dongli Gongcheng/Journal of Engineering for Thermal Energy and Power 16 (4) (2001) 403–405 (in Chinese).

[4] X.X. Huang, Double herringbone arch suitable for various coal with efficient smoke control and coal saving, Industrial Boiler 1 (1996) 2–4 (in Chinese).

[5] S.E. Hui, T.M. Xu, Z.J. Liu, et al., Countermeasures for the avoidance of positive-pressure in fire-bed boiler furnace, Reneng Dongli Gongcheng/Journal of Engineering for Thermal Energy and Power 9 (1) (1994) 14–17 (in Chinese).

[6] X.X. Huang, The "slight-explosion" phenomenon in stokers and its relations with arches – a new development in arch theory, Industrial Boiler 1 (1999) 18–20 (in Chinese).

[7] X.X. Huang, G.C. Lu, The discovery of "slight explosion phenomenon and study of anti-explosion arch in stoker firing, in: Z.H. Chen, T.N. Veziroglu, D.A. Reay (eds.), Proceedings of the International Conference on Energy and Environment, Shanghai, 1995.

[8] X.X. Huang, The detection and study of the "mini-explosion phenomenon in stoker firing, in: P.L. Ni, N.R. Li (eds.), Proceedings of CSPE-JSME-ASME International Conference on Power Engineering, vol. 1, Shanghai, 1995.

[9] J. Smagorinsky, General circulation experiments with the primitive equations. I. The basic experiment, Monthly Weather Review 91 (3) (1963) 99–164.

[10] D.K. Lilly, On the application of the Eddy viscosity concept in the inertial subrange of turbulence, NCAR Manuscript (1966) 123.

[11] A. Bakker, L.M. Oshinowo, E.M. Marshall, The use of large eddy simulation to study stirred vessel hydrodynamics, 10th European Conference on Mixing, July 2–5, 2000, pp. 247–254.

[12] A. Pentaris, S. Tsangaris, Numerical simulation of unsteady viscous flows using an implicit projection method, International Journal for Numerical Methods in Fluids 23 (1996) 897–921.

[13] X. Zhou, K.H. Luo, J.J.R. Williams, Vortex dynamics in spatio-temporal development of reacting plumes, Combustion and Flame 129 (1–2) (2002) 11–29.

[14] B. Wegner, Y. Huai, A. Sadiki, Comparative study of turbulent mixing in jet in cross-flow configurations using LES, International Journal of Heat and Fluid Flow 25 (5) (2004) 767–775.

[15] X.Y. Zhou, J.C.F. Pereira, Large Eddy simulation (2D) of a reacting plane mixing layer using filtered density function closure, flow, Turbulence and Combustion 64 (2000) 279–300.

[16] P. Cheng, Two-dimensional radiation gas flow by a moment method, AIAA Journal 2 (1964) 1662–1664.

[17] R. Siegel, J.R. Howell, Thermal radiation heat transfer, fourth ed., Taylor & Francis, New York, 2002.

[18] A. Coppalle, P. Vervisch, The total emissivities of high-temperature flames, Combustion and Flame 49 (1983) 101–108.

[19] T.F. Smith, Z.F. Shen, J.N. Friedman, Evaluation of coefficients for the weighted sum of gray gases model, Journal of Heat Transfer, ASME 104 (4) (1982) 602–608.

[20] R.D. Blevins, Flow-induced Vibration, Van Nostrand Reinhold Co., New York, 1977.

[21] H. Nishimura, Y. Taniike, Aerodynamic characteristics of fluctuating forces on a circular cylinder, Journal of Wind Engineering and Industrial Aerodynamics 89 (7–8) (2001) 713–723.

[22] D. Rocchi, A. Zasso, Vortex shedding from a circular cylinder in a smooth and wired configuration: comparison between 3D LES simulation and experimental analysis, Journal of Wind Engineering and Industrial Aerodynamics 90 (4–5) (2002) 475–489.